What Drives Plate Motion?

Yongfeng Yang

Bureau of Water Resources of Shandong Province
No. 127, Lishan Road, Jinan, Shandong Province, 250014, CHINA
E-mail: roufeng_yang@yahoo.com, roufengyang@gmail.com

Abstract

Plate motion is a remarkable Earth process and is widely ascribed to several driving forces: ridge push, slab pull, and basal drag. However, an in-depth investigation demonstrates that these forces are incomplete. Here, we propose that deep oceans generate pressure and that the application of this pressure against the walls of ocean basins, which are the sides of continents, may yield enormous horizontal forces (i.e., ocean-generated forces). The net effects of these forces provide lateral push to the continents and may cause them to move horizontally; further, the moving continents drag the crusts connected to them, which gives rise to plate motion. The estimate shows that ocean-generated forces may impel South America, Africa, India, and Australia to move 2.8, 4.2, 5.7, and 6.3 cm/yr, respectively, and the movement of the Pacific Plate may reach 8.9 cm/yr.

1 Introduction

One of the most significant achievements in the 20th century was the establishment of plate tectonics, which developed from the previous concept of continental drift (Wegener, 1915 and 1924). Plate tectonics mainly describes the motion of a dozen different-sized plates that connect with each other to form a giant "Jigsaw Puzzle" over the Earth's surface. The evidence supporting this motion includes shape fitting of the African and American continents, a coal belt crossing from North America to Eurasia, identical directions of ice sheet movement in southern Africa and India, and speed measurements made by the global positioning system (GPS). In addition, paleomagnetic reversals in oceans (Hess, 1962; Vine and Matthews, 1963) reflect sea-floor spreading, and studies of the Hawaii-Emperor seamount chain have shown that the chain is actually a trace of the lithosphere rapidly moving over relatively motionless hotspots (Wilson, 1963; Raymond, et al., 2000), further confirming

the Earth's surface motion. During the past 50 years, the understanding of plate motion has expanded greatly. The plates were found to have been periodically dispersed and aggregated in the Mesozoic, accompanied by 5~6 significant astronomical events (Cande et al., 1989; Cande and Kent, 1992; Ma et al., 1996; Burchfiel et al., 1992; Wan, 1993; Hibsch et al., 1995). The speed and direction of plate motion supported by paleomagnetism and deformation in the intraplate regions exhibited various styles over geological time (Wan, 2018). Global measurements of tectonic stresses revealed a strong correlation with plate motion, by which the forces acting on the plates may be constrained (Bott and Kusznir, 1984; Zoback et al., 1989; Zoback & Magee, 1991; Zoback, 1992; Richards, 1992; Sperner et al., 2003; Heidbach et al., 2007; Heidbach et al., 2010; Heidbach et al., 2016; Heidbach et al., 2018; Wan, 2018).

Exploring the driving forces behind plate motion is important because it provides the first insights into the processes that yield plate tectonics. Throughout the history of plate tectonics, a large variety of forces have been postulated to explain plate motion. Forces include centrifugal and tidal forces, ridge push, slab pull, basal drag, slab suction, mantle plume, geoid deformation, and the Coriolis force (Wegener 1915, Holmes, 1931; Pekeris, 1935; Hales, 1936; Runcorn, 1962a,b; Wilson, 1963; McKenzie, 1968; McKenzie, 1969; Morgan, 1971; Morgan, 1972; Turcotte and Oxburgh, 1972; Forsyth & Uyeda, 1975; Oxburgh and Turcotte, 1978; Spence, 1987; White & McKenzie, 1989; Richards, 1992; Vigny, et al., 1992; Bott, 1993; Tanimoto & Lay, 2000; Conrad & Lithgow-Bertelloni, 2002; Turcotte and Schubert, 2014). Slab pull derives from a cold, dense sinking plate that uses its own weight to pull the remaining plate it attaches to; ridge push is usually treated either as a body force or as a boundary force. As a body force, ridge push derives from the horizontal pressure gradient of the cooling and thickening of the oceanic lithosphere and acts over the area of the oceanic portion of a given plate. By contrast, as a boundary force, ridge push derives from a "gravity wedging" effect of warm, buoyant mantle upwelling beneath the ridge crest and acts at the edge of the lithospheric plate. As slab pull and ridge push act on the edges of plates, they are often termed boundary forces; basal drag (i.e., basal shear traction) is thought to be caused by the viscous moving asthenosphere along the bottom of the lithosphere; Mantle plume represents the rising hot mantle flow originated from the core-mantle boundary (Wilson, 1963; Morgan, 1971; Morgan, 1972;). Early studies of deformation modeling and torque balance analysis tended to agree that slab pull and ridge push are important for plate motion, whereas basal drag provides resistance other than driving (Solomon, et al., 1975; Forsyth & Uyeda, 1975; Chapple and Tullis, 1977; Richardson, et al., 1979; Wortel and Cloetingh, 1981; Richardson and Cox, 1984; Cloetingh and Wortel, 1986; Richardson and Reding, 1991; Stefanick and Jurdy, 1992). Subsequent studies with complicated physical models yielded an

improved understanding: buoyancy anomalies within the crust, the lithosphere, and the mantle act as the principal drivers, whereas the viscous dissipation at the base of and within the lithosphere and shear along thrust faults at collision zones resist plate motions (Lithgow-Bertelloni and Richards, 1995; Conrad and Hager, 1999; Becker and O'Connell, 2001; Zhong, 2001; Conrad and Lithgow-Bertelloni, 2002; Bird et al., 2008; Stadler et al., 2010; Becker and Faccenna, 2011; Ghosh et al., 2013; Coltice, et al., 2017). That is, in addition to slab pull and ridge push, the lithosphere and the mantle themselves feed plate motion in some way. For example, the lithosphere's density variation forms a lateral pressure gradient by which plate motion is driven; The sinking slab inserts into the deeper mantle, while at the same time, the hot mantle flows (i.e., plumes) originating from the core-mantle boundary rise up to the top of the asthenosphere; this process of upwelling and downwelling gives birth to a large-scale circulation of plate and mantle (i.e., whole mantle convection). A more detailed description of whole mantle convection may refer to these works (Bercovici, et al., 2015; Coltice, et al., 2017). On the whole, the efforts made in the past 40 years tend to agree that slab pull and ridge push are the primary driving forces for plate motions, whereas mantle plume acting as driver still remains controversial. Nevertheless, identifying these plate driving forces is still necessary and an ongoing subject among geophysicists.

Tectonic stress may provide strong constrains on plate driving forces. With the first release of the first- and second-order stress fields (Zoback et al., 1989; Zoback & Magee, 1991; Zoback, 1992), a feature in the World Stress Map (WSM) becomes evident that the orientation of the maximum horizontal compressional stress S_H in North America, South America and Europe are, at the plate scale, predominately subparallel to either the relative or absolute plate motions (Mu¨ller, et al., 1992; Richardson, 1992; Zoback, 1992). Due to this correlation of stress orientations and plate motions, the first-order intraplate stress patterns are thought to be the result of the same forces that drive plate motion, in particular ridge push, slab pull, trench suction, collisional forces, and traction at the base of the lithosphere [Go¨lke and Coblentz, 1996; Gru¨nthal and Stromeyer, 1992; Richardson, 1992; Zoback and Zoback, 1991; Zoback, 1992; Zoback and Burke, 1993; Zoback, et al., 1989]. Subsequent releases of the stress field and modeling studies reproducing plate tectonics support this conclusion (Sperner et al., 2003; Heidbach et al., 2007; Heidbach et al., 2010; Heidbach et al., 2016; Heidbach et al., 2018; Richards, 1992; Becker and O'Connell, 2001; Lithgow-Bertelloni and Guynn, 2004; Bird et al., 2008; Stadler et al., 2010; Ghosh and Holt, 2012; Alisic, et al., 2012; Ghosh, et al., 2013). This judgment, however, is not conclusive. Ascribing the first-order intraplate stress patterns to the same forces that drive plate motion is reasonable, because there must be forces behind plate motion. The forces acting on plate must first deform the plate if it is not rigid, and then, the forces that yield stress must be the same forces that drive plate motion. Nevertheless,

ascribing these stress patterns to these forces (e.g., ridge push, slab pull, trench suction) is still immature. Indeed, a good match in both orientation and style can be obtained between the stress yielded by these forces and the observed stress in the WSM (e.g., Lithgow-Bertelloni and Guynn, 2004; Ghosh, et al., 2013), but this match is only limited to a horizontal direction, and an examination across the whole lithospheric thickness is commonly absent. This lacking may lose very important clue on plate driving forces. In the latter section of this work, we shall demonstrate that these forces cannot be consistent with the observed tectonic stress.

Approximately 71% of the Earth's surface is covered with ocean, and the total volume of ocean is approximately 1.35 billion km^3, with an average depth of nearly 3,700 meters. The impact of such a large body of water on the Earth's crust must be significant. The ocean's weight is entirely borne by the crust; most importantly, ocean water (as liquid) exerts pressure on the wall of the ocean basin, which is the side of the continent. This pressure on the continent's side creates a force, and the connection of the continent to the crust allows this force to be laterally transferred to the crust. Unfortunately, this force has been completely overlooked by the geophysical community. In this work, we investigate this force with the hope of expanding our understanding of plate motion.

2 An ocean-generated force driving mechanism for plate motion

2.1 Forces acting on continents

A liquid can exert pressure on the wall of a container that holds it. According to Figure 1, the pressure generated at the wall of a cubic container may be written as $P=\rho g y/2$, and the application of this pressure across the wall yields a horizontal force. This force may be expressed as $F=PS=\rho g y^2 x/2$, where S is the wall's area, ρ and g are the liquid's density and gravitational acceleration, respectively, and x and y are the liquid's width and depth, respectively, in the container. Referring back to the real world, ocean basins are naturally very large containers, and their depths are often more than a few kilometers and vary from one place to another. All of these factors imply that oceans can generate enormous pressure everywhere and that this pressure is unequal between oceans. Furthermore, the application of pressure against the ocean basin's walls, which consist of the continents' sides, can yield enormous unequal forces on the continents. Geometrically, ocean pressure is always exerted vertical to the continental slope, by which a normal force is formed. This normal force is called ocean-generated force, which can be further decomposed into a horizontal force and a vertical force. Here, we define the continental crust, to which ocean pressure can be applied, as continent in the following sections. Subsequently, we list the plausible forces acting on a continent, as illustrated in Figure 1, and discuss the physical nature of these forces. The forces

acting on a continent can be classified into two categories: the forces acting on the parts of the continent that connect to oceans and those acting at both the bottom surface of the continent and the parts of the continent that connect to adjacent crust. The forces acting at the parts of the continent that connect to the ocean derive from ocean pressure and are treated as ocean-generated forces and denoted F_R at the right and F_L at the left. The horizontal forces decomposed from these forces are denoted F_R' at the right and F_L' at the left. The force acting at the bottom surface of the continent arises from a viscous coupling between the continent and underlying asthenosphere. It is called the basal friction force and denoted f_{base}. As addressed by Forsyth & Uyeda (1975), if there is active flow in the asthenosphere, such as thermal convection, f_{base} would act as a driving force (Runcorn, 1962a, b; Morgan, 1972; Turcotte & Oxburgh, 1972). If, on the other hand, the asthenosphere is passive with regard to plate motion, f_{base} would be a resistive force. Here, we assume f_{base} to be a resistive force. The forces acting on the parts of the continent that connect to adjacent crust arise from a physical binding of the continent and adjacent crust. Given that the continent moves towards the right, they are called the push force from the crust at the right side, the pull force from the crust at the left side, the shearing force from the crust at the far side, and the shearing force from the crust at the near side and denoted f_{right}, f_{left}, f_{far}, and f_{near}, respectively. Note that if there were no fractures (i.e., the gaps along ocean ridges and trenches at the subduction zones) around the ocean basin, ocean-generated forces may be balanced out by the basin itself. Forsyth & Uyeda (1975) showed that the world's extensional boundaries represented by fractures may reach up to 50,000 km. The fractures in the ocean basins allow ocean-generated forces to interact with basal friction. Then, a combination of all these forces for the continent in the horizontal direction may be written as

$$F = (F_L' - F_R') - (f_{base} + f_{right} + f_{left} + f_{far} + f_{near}) \quad (1)$$

where the first term ($F_L' - F_R'$) denotes the net horizontal force, which provides a dynamic source for the continent, and the second term ($f_{base} + f_{right} + f_{left} + f_{far} + f_{near}$) denotes the total resistive force, which hinders the continent's movement. Here, we indicate ($F_L' - F_R'$) as $F_{horizontal}$ and ($f_{base} + f_{right} + f_{left} + f_{far} + f_{near}$) as $F_{resistive}$. F_L' and F_R' may be further written as $F_L' = 0.5\rho g L h_L^2$, $F_R' = 0.5\rho g L h_R^2$, where ρ, g, L, h_L, and h_R are the density of water, gravitational acceleration, ocean width that fits the continent's width, ocean depth at the left, and ocean depth at the right.

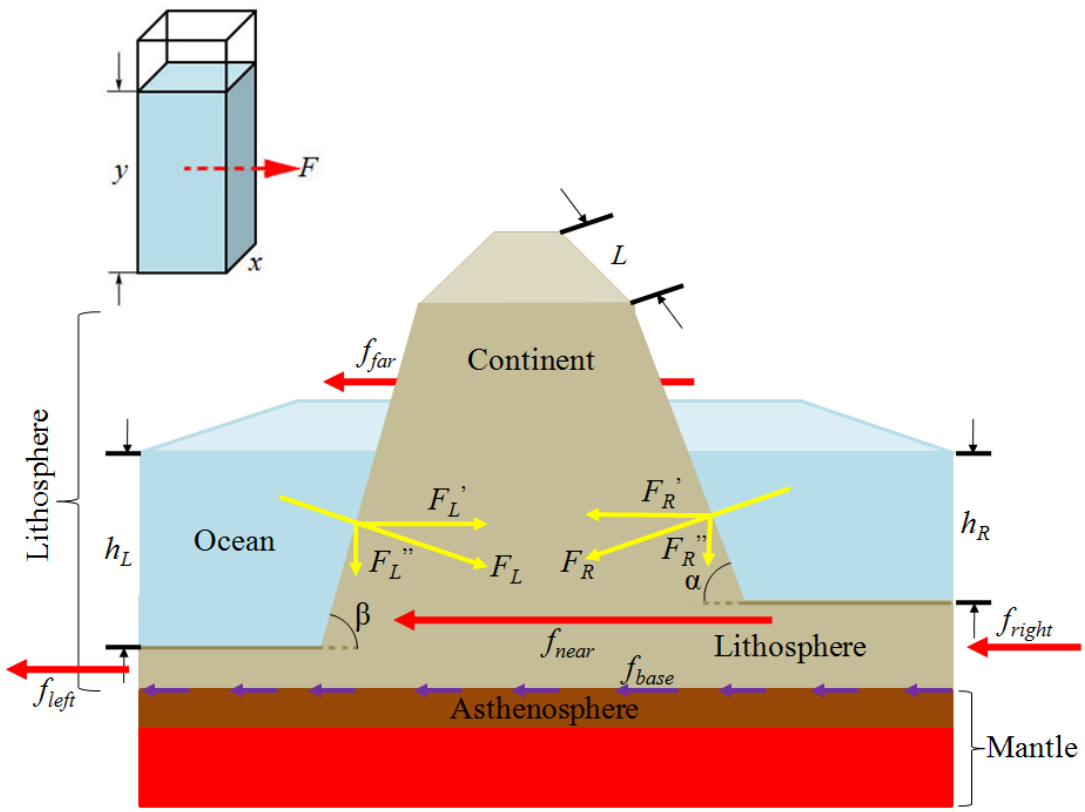

Fig. 1. Modeling the dynamics of a continent. $F_L(F_R)$ represents the ocean-generated force on the left (right) side of the continent, while F_L'(F_R') and F_L''(F_R'') denote the horizontal and vertical forces decomposed from the ocean-generated force, respectively. The term f_{base} denotes the basal friction force exerted by the asthenosphere, while f_{right}, f_{left}, f_{far}, and f_{near} denote the push force from the crust at the right side, the pull force from the crust at the left side, the shearing force from the crust at the far side, and the shearing force from the crust at the near side of the continent, respectively. The continent is assumed to move towards the left. L denotes the width of the continent's side; h_L and h_R are the ocean's depth at the left and right, respectively. α and β denote the inclinations of the continent's slope on either side. Note that ocean depth is highly exaggerated with respect to the lithospheric thickness.

2.2 Continental movement

Equation (1) provides three possibilities for the continent. If the net horizontal force is always less than or equal to the total resistive force, the combined force is less than or equal to zero, and the continent would remain motionless; if the net horizontal force is always greater than the total resistive force, the combined force is greater than zero, and the continent would be subject to an accelerating motion. Practically, it is impossible for the continent to undergo such a movement; and if the net horizontal force is sometimes greater than the total resistive force but other times less than the total resistive force, the combined force would be

discontinuous, and the continent would undergo discontinuous motion. We assume that there exists a weak balance between the net horizontal force and the total resistive force, and this balance can be periodically broken by an unusual event. The existence of this weak balance is discussed later. Most oceans experience two cycles of high and low water per day; these movements of water are the tides we know in everyday life. The tides cause oceans to oscillate vertically, which leads ocean pressure to vary periodically. Ocean pressure variations have been well confirmed by bottom pressure measurements (Figure 2). The variance in ocean pressure yields varying horizontal forces and thus provides the possibility for the net horizontal force to be discontinuously greater or less than the total resistive force. Then, the continent's movement may be outlined as in Figure 3: at stage t_1, the net horizontal force begins to increase, but since $F_{horizontal} - F_{resistive} < 0$, the continent remains motionless. At stage t_2, $F_{horizontal} - F_{resistive} > 0$, the continent accelerates, and its speed reaches its highest level at the end of this period. At stage t_3, $F_{horizontal} - F_{resistive} < 0$, the continent begins to decelerate until its speed becomes zero at the end of this period. At stage t_4, because $F_{horizontal} - F_{resistive} < 0$, the continent remains motionless. At stages t_5 and t_6, the continent moves similarly to the movements in stages t_2 and t_3, but at stage t_7, the continent again remains motionless. Simply, the continent discontinuously achieves some forward movement at stages t_2, t_3, t_5, and t_6 and some stagnation at stages t_1, t_4, and t_7. This movement and stagnation in total provide a net forward movement for the continent during the day. Expanding this day to one year, the continent moves steadily forward during the year. Further, extending this year to a timescale of millions of years and considering that the oceans are extensively distributed around the globe, we conclude that the continents could have moved steadily forward over millions of years. Figure 4 exhibits the global distribution of the oceans and the resultant horizontal forces around the continents.

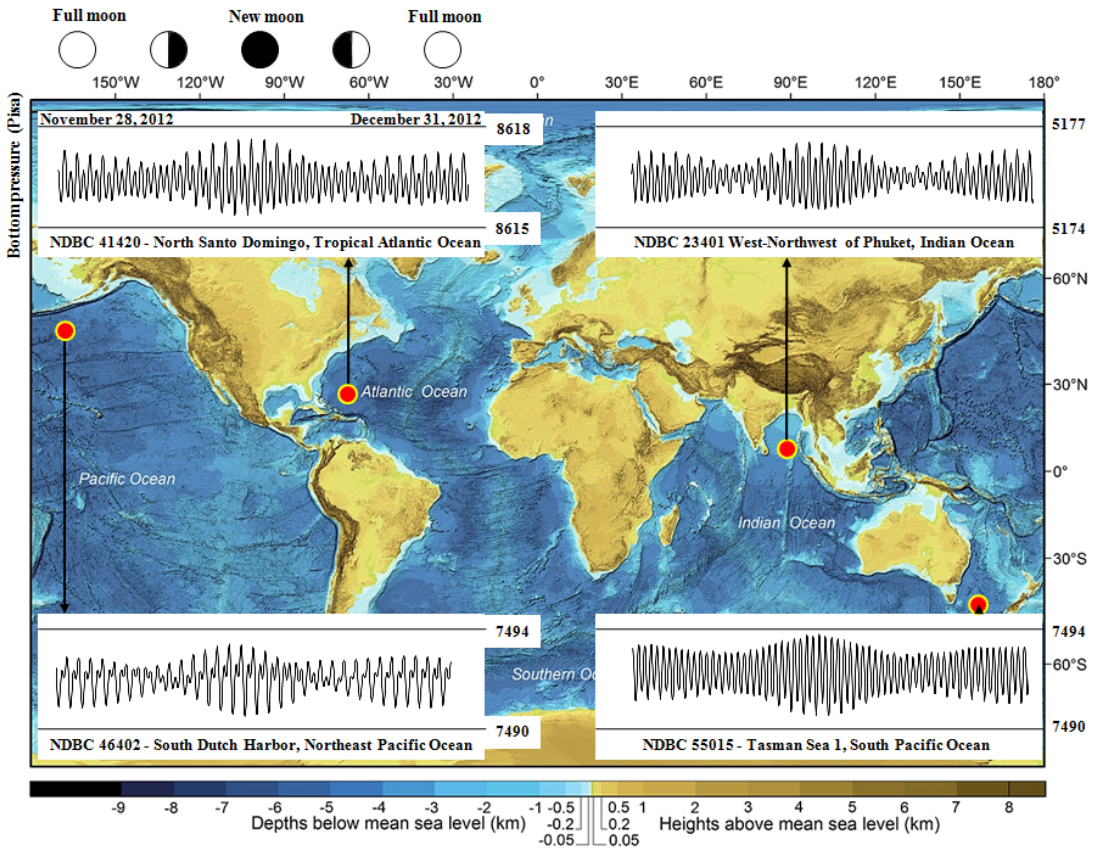

Fig. 2. Typical 1-month bottom pressure changes during 2012. Bottom pressure data are from the National Oceanic and Atmospheric Administration (NOAA) National Data Buoy Center. The background reflects the GEBCO_2014 grid (Weatherall et al., 2015), and the colors denote ocean floor (blues) and land (browns).

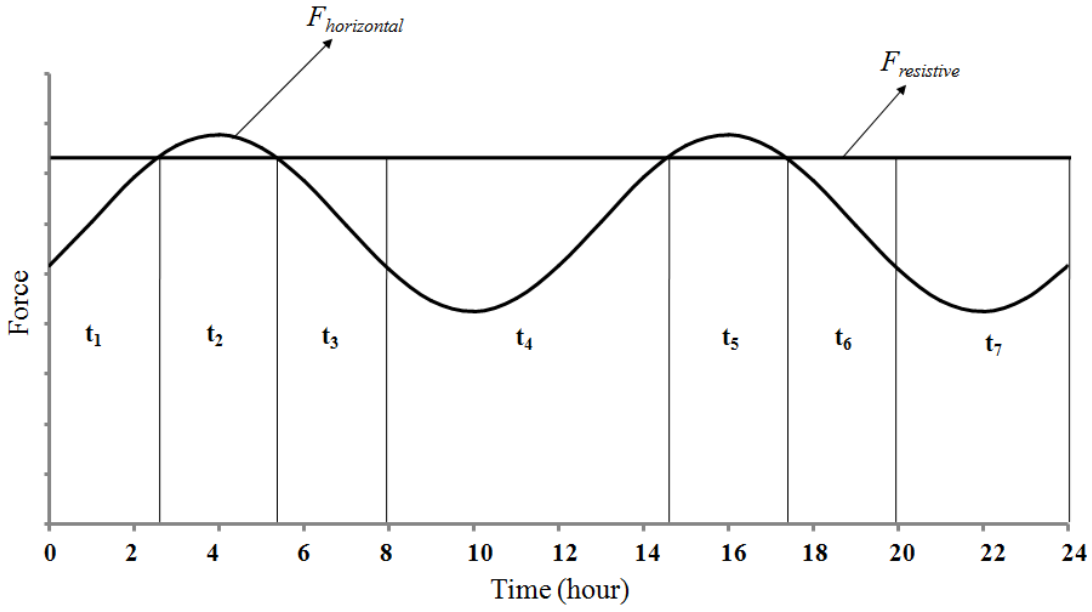

Fig. 3. Dynamic analysis for the continent. $F_{horizontal}$ denotes the net horizontal force generated

for the continent, and $F_{resistive}$ denotes the total resistive force acting on the continent. Note that the oscillation of the net horizontal force is somewhat exaggerated.

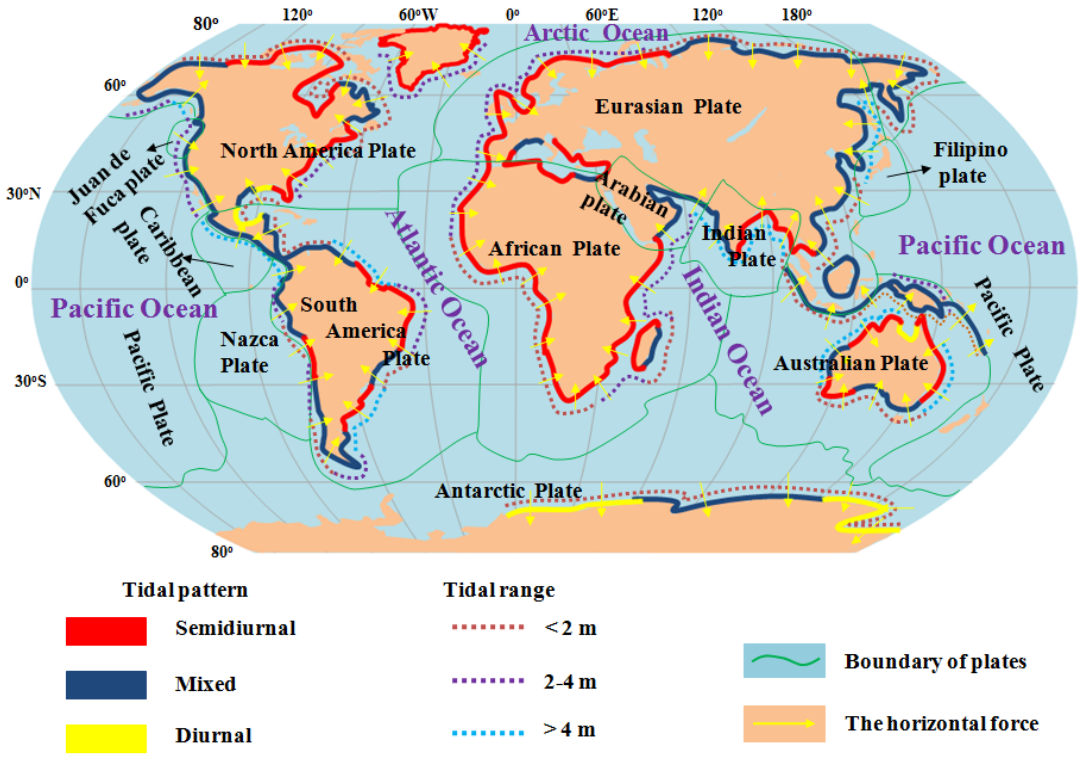

Fig. 4. Global view of the distribution of tidal patterns, tidal ranges, plate tectonics, and the horizontal forces generated for continents. The supporting tidal data are from U.S. NOAA, the GLOSS database from the University of Hawaii Sea Level Center (Caldwell et al. 2015), and the Bureau National Operations Center (BNOC) of Australia; tide ranges also refer to the Times Atlas of the Oceans, 1983, Van Nostrand Reinhold, NY.

A quantitative resolution of the continent's movement must consider additional details. Most continents are surrounded by oceans, which means that the net horizontal force exerted on a continent is a consequence of the combination of the horizontal forces generated on all the sides of this continent. The Earth's curved surface means that the horizontal forces generated do not lie in a plane. Additionally, the tides surrounding a continent are not synchronous, and their amplitudes display two cycles per month. This rhythm is thought to be related to the positions of the Sun, Moon, and Earth. For example, the tides become maximum at the times of full and new moons and become minimum at the times of first quarter and last quarter. Furthermore, the tidal loading/unloading rate is not uniform. More features of the tides may be found in these works (Pugh 1987; Pugh and Woodworth 2014). To simplify our model, we assume the continent to be rigid and its surface flat, which allows us to apply Newtonian mechanics. We further assume the tides around a continent to be synchronous and their amplitudes to be constant during a month. The tidal loading/unloading rate is assumed to be

linear, which enables us to easily infer that the time taken by the continent to accelerate is the same as that to decelerate, namely, t_2=t_3. Then, according to Newton's 2nd law, and given two tides per day, the distance that a continent moves during a year may be approximately written as

$$D = \mathbf{365 * 2 *} \frac{1}{2} * \frac{(F_{horizontal-\max} - F_{resistive})}{M} * t^2 \qquad (2)$$

where $F_{horizontal\text{-}\max}$ denotes the net horizontal force generated at the time of highest tide, $F_{resistive}$ denotes the total resistive force, M denotes the continent's mass and may be obtained through M=Sd$\rho_{continent}$ (where S, d, and $\rho_{continent}$ are the continent's area, thickness, and density, respectively) and t is the time that the continent takes to accelerate during a tide. Because the horizontal forces exerted on the continent are often along different directions, we need to combine these forces into a resultant horizontal force. We first decompose each of the horizontal forces into latitudinal and longitudinal components. Subsequently, by simple addition, all of the latitudinal and longitudinal components are separately combined into a latitudinal force and a longitudinal force. Furthermore, the latitudinal and longitudinal forces are combined into a final horizontal force. The net horizontal force may be written as $F_{horizontal-\max} = \left((\sum_{i=1}^{n} F_{i-horizontal-latitudinal})^2 + (\sum_{i=1}^{n} F_{i-horizontal-longitudinal})^2 \right)^{\frac{1}{2}}$, where $F_{i\text{-}horizontal\text{-}latitudinal}$ and $F_{i\text{-}horizontal\text{-}longitudinal}$ are the latitudinal and longitudinal components that are derived from the horizontal force, respectively. These components can be expressed as $F_{i-horizontal-latitudinal} = F_{i-horizontal} \sin\Omega_i$ and $F_{i-horizontal-longitudinal} = F_{i-horizontal} \cos\Omega_i$. Ω_i denotes the inclination of the ith side to latitude (+) and may be obtained through the geographic latitudes and longitudes of the two ends of this side. $F_{i\text{-}horizontal}$ denotes the horizontal force generated at the ith side of the continent at the time of highest tide and can be written as $F_{i\text{-}horizontal}$ = 0.5ρgL(h_{ocean}+h_{tide})^2. Here, ρ, g, L, h_{ocean}, and h_{tide} are the density of water, the gravitational acceleration, the continent side's width, the ocean depth that connects to the continent side, and the tidal height, respectively. Tidal height may be expressed as h_{tide}=Asinωt, where A is tidal amplitude and ω and t are the angular frequency and time, respectively.

In practice, the continent's side is not flat, and the continent's base is generally wider than its top, making the continent look more like a circular truncated cone standing in the ocean. As the horizontal force generated is related to the ocean's width (i.e., the continent side's width), we need to horizontally project the continent into a polygonal column and dissect the whole

side of this column into a series of smaller rectangular sides connecting one to another and subsequently to calculate the horizontal force generated at each of these rectangular sides. Finally, we combine these horizontal forces to form a single horizontal force. With these theoretical ideas, we take the parameters involved to estimate the movement of a few continents (South America, Africa, India, and Australia). The controlling sites used to determine the lengths of sides refer to Figure 5, and the longitudes and latitudes of these sites were obtained through Google Earth software. The parameters involved and the horizontal forces generated are separately listed in Tables 1 and 2. Please note that the determination of the time taken by the continent to accelerate and decelerate during a tide is rather complicated. Mathematically, if these parameters (tidal height, ocean depth, ocean width, and total resistive force, for example) can be given, we may refer to Figure 3 to develop a nonlinear relationship resolving the time. As we are estimating the continent's movement, a nonlinear relationship is not considered here; instead, we choose to estimate the time. Finally, the South American, African, Indian, and Australian continents realize movements of 2.8, 4.2, 5.7, and 6.3 cm/yr, respectively (Table 3), given that the times taken by them to accelerate within a tide are 197, 165, 145, and 176 s, respectively. These results are consistent with the observed movement of approximately 5.0~10.0 cm/yr (Read and Watson 1975).

Note that the resistive force ($F_{resistive}$) used in the calculation is technically valued. Undoubtedly, this treatment deserves a discussion. As shown in Figure 1, the total resistive force includes four components: the basal friction force, the push force, the pull force, and the shearing forces. The push, pull, and shearing forces essentially originate from the basal frictions exerted by the asthenosphere on the lithosphere. The basal friction is determined by a few factors: the asthenosphere's viscosity, the continent's area, the continent's speed, and the asthenosphere's thickness. The area and speed can be exactly measured, but the viscosity and thickness of the asthenosphere remain highly uncertain. Cathless (1971) concluded that the viscosity is no less than 10^{20} P, and Jordan (1974) treated the thickness as 300 km. Fjeldskaar (1994) suggested that the asthenosphere has a thickness of less than 150 km and a viscosity of less than 7.0×10^{20} P. Some authors using glacial isostatic adjustment and geoid studies concluded that the asthenospheric viscosity ranges from 10^{19} to 10^{21} P (Hager and Richards, 1989; King, 1995; Mitrovica, 1996). James et al. (2009) used a model to show that the asthenospheric viscosity varies from 3×10^{19} P for a thin (140 km) asthenosphere to 4×10^{20} P for a thick (380 km) asthenosphere. These factors completely imply that the total resistive force cannot be exactly known and must be estimated.

Also note that our understanding of the continent's movement relies on assuming a weak balance between the net horizontal force and the total resistive force. This balance also

deserves a discussion of feasibility. The basal friction exerted by the asthenosphere along the continent's base can be expressed as $F_A=\mu Au/y$, where μ, A, u, and y are the viscosity of the asthenosphere, the continent's area, the continent's speed, and the thickness of the asthenosphere, respectively. Here, we adopt $\mu= 3\times10^{19}$ P and y=200 km to estimate the basal friction forces acting upon the four continents (South America, Africa, India, and Australia). The speeds of these continents are assumed to be 2.7, 4.2, 5.6, and 6.4 cm/yr, respectively, and the areas of these continents are listed in Table 1. The basal friction forces estimated are listed in Table 2. For each of these four continents, the magnitude of the horizontal force generated is extremely close to that of basal friction. This result may not be coincidental because these two forces are obtained through two different methods. Finally, we find that there may be a weak balance between the net horizontal force and the total resistive force.

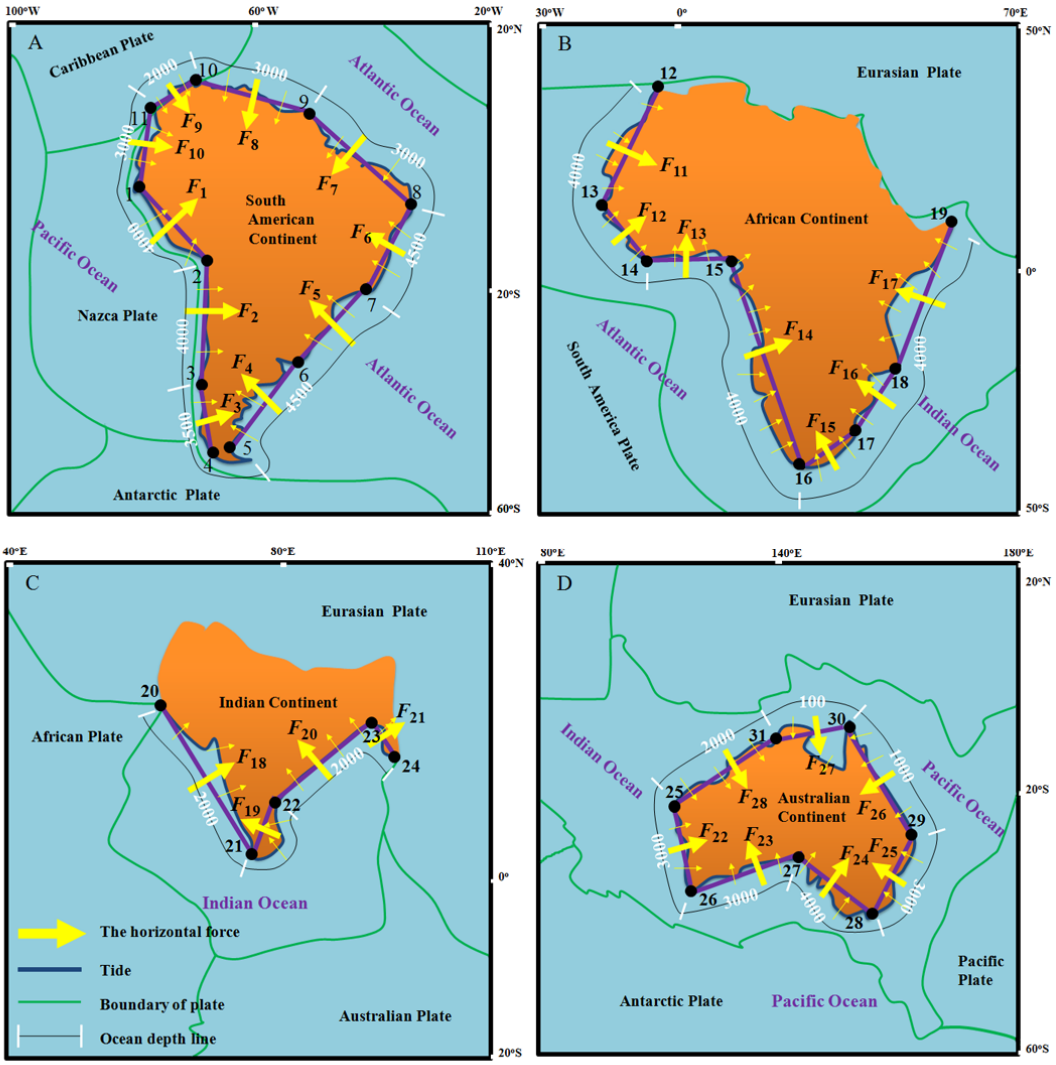

Fig. 5. Geographic treatment of the controlling sites for the four selected continents and the horizontal forces generated for them. *F* (yellow arrows) denotes the horizontal force generated,

while purple bars denote the distances affected by the horizontal forces. The product of this distance and ocean depth is the area to which the horizontal force applies. The dots with numbers denote the controlling sites. Ocean depths were artificially resolved from Google Earth software.

Table 1 Basic information for the four selected continents

Continent	Area	Thickness	Density	Mass	Site			Site to site				Tidal height	Ocean depth
								distance		inclination to latitude, east (+)			
	S	d	ρ	M				L		i	Ω_i	h_{tide}	h_{ocean}
	km^2	km	kg/m^3	kg	No.	Longitude	Latitude	km			degree (°)	m	m
South America	17,840,000	6	3,100	3.32E+20	1	80.0°W	2.0°S	1_2	2,087	1	122.01	1.5	4,000
					2	70.0°W	18.0°S	2_3	1,153	2	73.30	1.5	4,000
					3	73.0°W	28.0°S	3_4	2,780	3	90.00	1.5	3,500
					4	73.0°W	53.0°S	5_6	2,308	4	51.15	2.0	4,500
					5	68.0°W	52.5°S	6_7	1,730	5	43.78	2.0	4,500
					6	54.0°W	34.5°S	7_8	1,952	6	64.89	1.5	4,500
					7	42.0°W	23.0°S	8_9	2,525	7	146.66	1.5	3,000
					8	34.0°W	7.0°S	9_10	2,157	8	160.64	1.5	3,000
					9	53.0°W	5.5°N	10_11	836	9	41.26	1.5	2,000
					10	72.0°W	12.0°N	11_1	1,033	10	75.66	1.5	3,000
					11	78.0°W	7.0°N						
Africa	30,370,000	6	3,100	5.65E+20	12	6.0°W	35.5°N						
					13	17.0°W	14.7°N	12_13	2,535	11	117.65	1.0	4,000
					14	7.0°W	4.6°N	13_14	1,531	12	45.00	1.0	4,000
					15	8.0°E	4.4°N	14_15	1,696	13	3.81	1.0	4,000
					16	22.2°E	34.7°S	15_16	4,577	14	109.75	1.0	4,000
					17	30.4°E	30.7°S	16_17	886	15	26.00	1.0	4,000
					18	40.0°E	16.0°S	17_18	1,904	16	56.85	1.0	4,000
					19	51.0°E	11.0°N	18_19	3,237	17	67.83	1.0	4,000
India	4,400,000	6	3,100	8.18E+19	20	66.8°E	25.0°N						
					21	77.5°E	8.0°N	20_21	2,205	18	122.19	2.0	3,000
					22	80.0°E	15.2°N	21_22	846	19	70.85	2.0	3,000
					23	91.5°E	22.7°N	22_23	1,468	20	33.11	2.0	3,000
					24	94.3°E	16.0°N	23_24	801	21	112.68	2.0	3,000

					25	114.0°E	23.0°S	25_31	2,162	28	32.43	2.0	2,000
					26	117.2°E	35.0°S	25_26	1,370	22	104.93	2.0	4,000
					27	131.0°E	31.5°S	26_27	1,340	23	14.23	1.0	5,000
Australia	8,600,000	6	3,100	1.60E+20	28	149.8°E	37.6°S	27_28	1,846	24	162.02	1.0	5,000
					29	153.0°E	25.4°S	28_29	1,390	25	75.30	2.0	3,000
					30	142.4°E	10.8°S	29_30	1,970	26	125.98	2.0	1,000
					31	131.0°E	12.2°S	30_31	1,252	27	7.00	2.0	100

Notes: All geographic sites refer to Figure 5; tidal height is half of the tidal range.

Table 2 The generated horizontal force and constrained parameters for the four selected continents

Continent	i	Horizontal force [a]			$F_{horizontal\text{-max}}$	Resistive force [b]	Friction [c]	Time taken to accelerate during a tide [d]
		horizontal	decomposed					
			latitudinal, east (+)	longitudinal, north(+)				
		$F_{i\text{-}horizontal}$	$F_{i\text{-}horizontal\text{-}latitudinal}$	$F_{i\text{-}horizontal\text{-}latitudinal}$				
		N(*10^{17})				N(*10^{17})		Second
South America	1	1.6375	1.3886	0.8679				
	2	0.9050	0.8668	-0.2600				
	3	1.6701	1.6701	0.0000				
	4	2.2925	-1.7853	1.4382				
	5	1.7184	-1.1890	1.2406				
	6	1.9378	-1.7546	0.8225				
	7	1.1148	-0.6127	-0.9313				
	8	0.9520	-0.3156	-0.8981				
	9	0.1642	0.1083	-0.1234				
	10	0.4559	0.4417	-0.1129				
			-1.1817	2.0434	2.3605	2.3604	2.2911	197.18
Africa	11	1.9883	1.7613	-0.9226				
	12	1.2006	0.8489	0.8489				
	13	1.3304	0.0885	1.3275				

	14	3.5900	3.3789	1.2129				
	15	0.6953	-0.3048	0.6249				
	16	1.4932	-1.2502	0.8164				
	17	2.5392	-2.3515	0.9580				
			2.1711	4.8662	5.3285	5.3283	6.0670	165.14
India	18	0.9737	0.8241	0.5187				
	19	0.3734	-0.3527	0.1225				
	20	0.6482	-0.3541	0.5430				
	21	0.3536	0.3263	0.1363				
			0.4435	1.3205	1.3930	1.3929	1.1720	144.59
Australia	22	1.0751	1.0388	0.2770				
	23	1.6417	-0.4036	1.5914				
	24	2.2627	0.6983	2.1523				
	25	0.6137	-0.5936	0.1557				
	26	0.0969	-0.0784	-0.0569				
	27	0.0006	0.0001	-0.0006				
	28	0.4246	0.2277	-0.3584				
			0.8892	3.7604	3.8641	3.8640	2.5771	175.62

Notes: All horizontal forces generated refer to Figure 5;

a (the horizontal force) and *c* (the basal friction) are calculated, while *b* (the total resistive force) and *d* (the time taken to accelerate during a tide) are technically valued.

Table 3 The resultant movements for the four selected continents

Continent	Movement per year	To latitudinal direction, east (+)
	mm/yr	degree
South America	27.59	120.04
Africa	41.85	65.96
India	56.46	71.44
Australia	63.09	76.70

The above treatment of the continent's movement is idealized. Because most of the horizontal forces exerted on the continent are along different directions and cannot pass the barycenter of the continent, this situation may produce a torque to rotate the continent. Figures 6 (A and B) conceptually demonstrate how these continents (North America and Eurasia, for example) move under the torque produced by the horizontal forces.

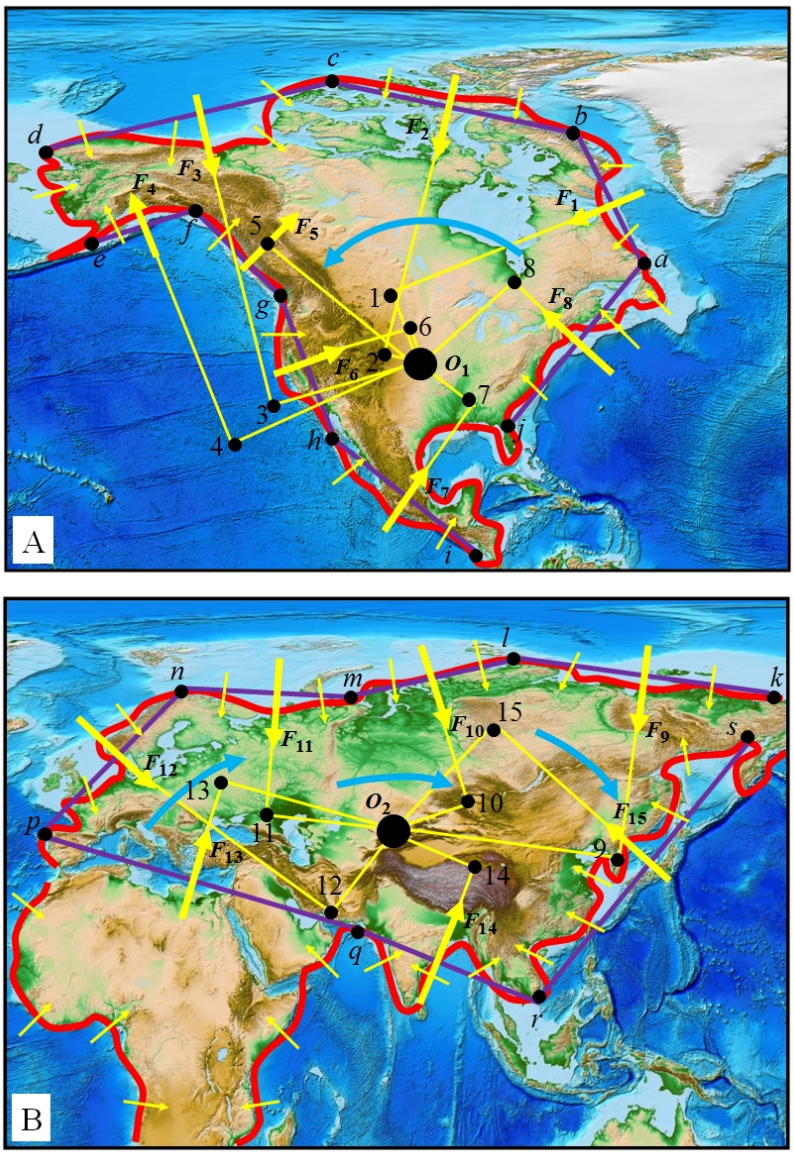

Fig. 6. Dynamics for the rotation of the North American and Eurasian continents. O_1 and O_2 denote possible positions of the barycenters of the two continents. F_1, F_2, and F_3, i.e., marked with yellow arrows, denote the horizontal forces generated; *a*, *b*, and *c*, e.g., denote the selected controlling sites, while *ab*, *bc*, *cd*, i.e., marked with purple bars, denote the lengths of the continents' sides; $O_1$1, $O_1$2,. ..,$O_2$9, and $O_2$10 denote the arms to which the horizontal forces are applied. The torque effect is a product of force and arm. Curved blue arrows represent expected rotations around these barycenters. Note that F_{13} represents a lateral push force from the traveling

African continent. The background map was obtained from the ETOPO1 Global Relief Model (Amanteand Eakins, 2009).

2.3 Plate motion

Plate motion may be a consequence of the horizontal force. Referring to Tables 1 and 2, the majority of the net horizontal force is used to oppose the total resistive force, which is composed of the basal friction exerted by the asthenosphere, the push force from the crust on the right side, the pull force from the crust on the left side, the shearing force from the crust on the far side, and the shearing force from the crust on the near side. By the principle of action and reaction, these resistive forces may further drive the crusts that bear them to move. We believe that these interactions ultimately create plate motion over the globe.

Force from one plate on another may be exemplified with the motion of the Pacific Plate. As outlined in Figure 7, the Australian Plate and the North American Plate independently provide push forces F_{PA} and F_{PN} on the Pacific Plate; a combination of these two forces is the force F_P, which provides dynamics for the Pacific Plate. A quantitative treatment of the motion of the Pacific Plate is relatively complicated. The Pacific Plate is first considered to be rigid and flat. These assumptions allow deformation to be negligible and related forces to interact in a plane. According to the relationship between movement and force, Equation (2) can be simplified as $F \sim DM$, where F, M, and D are the force that acts on a continent, the continent's mass, and the continent's movement, respectively. Applying this simplified equation to the South American continent, the force is $F_S \sim D_S M_S$. Furthermore, if we apply this equation to the North American continent in analogy with the South American continent, the force is $F_N \sim F_S D_N M_N / D_S M_S$, where F_N and F_S denote the net horizontal forces obtained by the North American and South American continents, respectively; D_N and D_S are the movements of these two continents, respectively; and M_N and M_S denote their masses. Referring to the parameters listed in Tables 1, 2, and 3, the values are $F_S=2.3605\times10^{17}$ N, $D_S=2.7$ cm per year, and $M_S=3.32\times10^{20}$ kg. The North American continent has an area of approximately 24,709,000 km^2, and according to another expression, $M=S\mathrm{d}\rho_{continent}$ (where S, d, and $\rho_{continent}$ are the continent's area, thickness, and density, respectively); thus, the continent's mass may be $M_N=4.60\times10^{20}$ kg. The North American Plate rotates counterclockwise and moves at a speed of approximately 1.5~2.5 cm per year. Here, we adopt $D_N=2.0$ cm per year for the western portion of this plate that interacts with the Pacific Plate. Then, the net horizontal force calculated for the North American continent would be $F_N=\sim2.4227\times10^{17}$ N. To drivethe North American Plate to move, the net horizontal force F_N must overcome the total resistive force, which mainly consists of the push force from the Pacific Plate and the shearing force from the South American Plate. The push force and the shearing force derive from the basal

friction exerted by the asthenosphere. Referring to the basal friction expression $F_A=\mu Au/y$, the push force provided by the Pacific Plate can be written as $F_{PN}= F_N S_P/(S_P+S_N)=1.0261\times10^{17}$ N, where S_P and S_N are the areas of the Pacific Plate and South American Plate, respectively. Referring to Table 2, the total resistive force for the Australian plate is $F_{Au\text{-}resistive}$ $=3.8640\times10^{17}$ N; given that 25% of this resistive force is used to overcome the push force from the Pacific Plate, the push force is $F_{PA}=9.6600\times10^{16}$ N. The Australian Plate moves dominantly in the northeast direction, and the inclination of this direction to latitude (+) is approximately 76.7°, as listed in Table 3. Most of the North American Plate moves in an approximately southwest direction away from the Mid-Atlantic Ridge, and we assume the push force from the North American Plate is oriented along a southwest direction. The inclination of this direction to latitude (+) is approximately 190°. Subsequently, the net horizontal force on the Pacific Plate can be written as $F_P=((F_{PN}^2+F_{PA}^2-2\times F_{PN}\times F_{PA}\times\cos(\alpha-\beta))^{0.5}$, and $\cos\gamma=(F_P^2+F_{PN}^2-F_{PA}^2)/(2\times F_P\times F_{PN})$, where $\alpha=76.7°$ and $\beta=10°$. Finally, the force is $F_P=1.096315\times10^{17}$ N, and $\gamma=54.03°$. Similarly, we assume that a majority of the net horizontal force on the Pacific Plate is used to overcome the total resistive force, which mainly consists of the friction exerted by the asthenosphere along the Pacific Plate's base. Referring to Table 2, the ratio of the total resistive force and the net horizontal force for the South American continent may reach 0.99999907. This amplitude allows us to consider a ratio of 0.99999 for the Pacific Plate; then, the total resistive force for the Pacific Plate is $F_{Pa\text{-}resistive}=1.096304\times10^{17}$ N. The continental crust's thickness is given as 6.0 km, and referring to Table 1, the average ocean depth is less than 4.0 km. These two numbers allow us to accept a remaining thickness of 2.0 km for the continental crust to contact the oceanic crust. The mass of the Pacific Plate may be written as $M_{Pacific}=Sd\rho_{plate}$ (where S, d, and $\rho_{plate}$are the plate's area, thickness, and density, respectively). Given that the continent's density is the same as the plate's density, we adopt the Pacific Plate's area as 103,300,000.00 km^2; then, the value is $M_{Pacific}= 6.4046\times10^{20}$ kg. Applying Equation (2) and giving the plate a time of 1,194.45 s during a tide to accelerate it, the Pacific Plate finally may show a movement of 89.44 mm per year, approximately along the northwest direction.

The North American Plate presently rotates counterclockwise; if we look back in time, it must have rotated substantially over a timescale of more than millions of years. In the past, the push force F_{PN} likely did not exist, and the Pacific Plate was pushed by the Australian Plate alone to move along a northeast direction. This sequence requires an abrupt change in motion for the Pacific Plate to have occurred when the North American Plate rotated to a central angle, from which a combination of the two lateral forces mentioned above is realized. Such a plate motion change has been supported by the Hawaiian–Emperor bend (Sharp and Clague, 2006; Wessel and Kroenke, 2008).

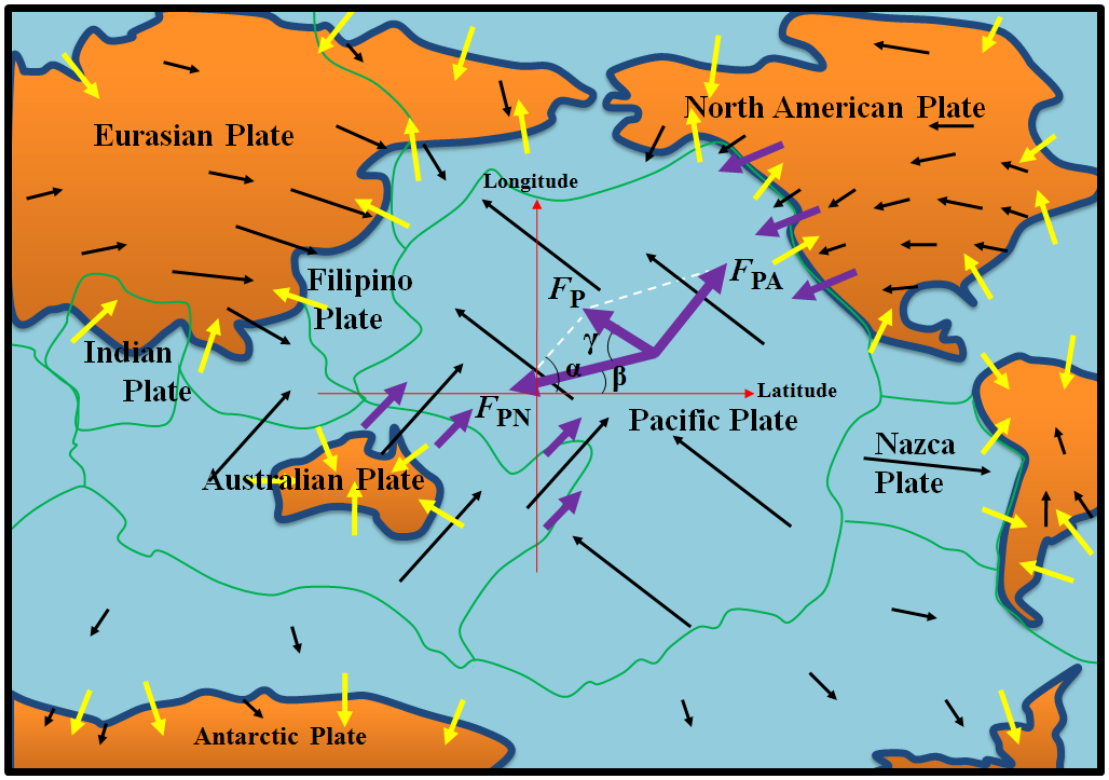

Fig. 7. Modeling the dynamics of the Pacific Plate. Black, yellow, and purple arrows denote plate motions, horizontal forces generated due to oceans, and lateral push forces from related plates, respectively. Note that the lateral push force F_{PN}(F_{PA}) is approximately parallel to the motion of the North American (Australian) Plate.

3 Comparison of the ocean-generated force and the boundary forces

3.1 Magnitude

The ocean-generated force may be approximately expressed as $F = g\rho_w l^2 L/2$, where l and L are the depth and width of the ocean, respectively; given a depth of 5 km and a width of 300,000 km, which is equivalent to the total length of coastline, the total ocean-generated force would be 3.75×10^{19} N. The ridge push force is estimated to be on the order of 3×10^{12} N/m of ridge boundary (e.g., Haper, 1975; Lister, 1975; Parsons and Richter, 1980), and the slab pull force is estimated to be nearly one order of magnitude larger than the ridge push force (e.g., Turcotte and Schubert, 1982). Given a global ridge length of 50,000 km, the total ridge push force generated would be 1.5×10^{21} N. According to Wu et al. (2008), the magnitude of the slab pull force is estimated to be nearly 4.6×10^{13} N/m, the total width of the 207 subduction zones that they employed in the study is 49,657 km, and the total slab pull force generated reaches up to 2.27×10^{21} N. Immediately, some authors would infer that, since the total slab pull force and the total ridge push force exceed the total ocean-generated force by two orders of magnitude, these boundary forces must be the primary plate driving forces. This conclusion, however, is not correct. Let us investigate the applicability of these three forces. Based on

Turcotte and Schubert (2014), the resistance exerted by the asthenosphere along the lithosphere's base may be expressed as $F_A=\mu Au/y$, where μ and y are the asthenosphere's viscosity and thickness, respectively, and A and u are the lithosphere's area and speed, respectively. James et al. (2009) showed that the asthenospheric viscosity varies from 3×10^{19} P for a thin (140 km) asthenosphere to 4×10^{20} P for a thick (380 km) asthenosphere. Given $\mu=3\times10^{19}\sim 4\times10^{20}$ P, $A=5.1\times10^{8}$ km^2, u=6.0 cm/yr, and y=140~380 km, the resistance generated would be $2.09\times10^{19}\sim1.03\times10^{20}$ N. This number may represent the upper limit because part of the lithosphere moves at a lower speed. Comparing this resistance with these forces above, each of them can drive the lithosphere to move. Nevertheless, we must emphasize that from the viewpoint of dynamics, if the driving force an object accepts is greater than the resistance it accepts, the final result is accelerating motion for the object. If the driving force is less than the resistance, the final result is motionless, and if the driving force is equal to the resistance, the final result is uniform motion. As plates are steadily moving over the Earth's surface, this steady movement may be treated as uniform motion. If either the ridge push force or the slab pull force exceeds the resistance by one order of magnitude, it yields uniform motion for the plate with difficulty. Some authors would also argue that the net ridge push force combines with the net slab pull force to greatly oppose each other, the resultant force may reach the magnitude of the resistance; then, yielding uniform motion for the plate becomes possible. However, a real problem is that the ridge push force acts on the continental plate, while the slab pull force acts on the oceanic plate, this separation of distribution between these two forces makes their combination extremely difficult. By contrast, the total ocean-generated force is almost equivalent in magnitude to the resistance, and this forces easily yields uniform motion for the plate.

3.2 Stress

Tectonic stresses are caused by the forces that act on the plates (Middleton and Wilcock, 1996), and thereby they may used to constrain the plate driving forces. As mentioned earlier, a good match in both orientation and style has been obtained between the stress yielded by the established plate driving forces and the observed stress in the WSM (e.g., Lithgow-Bertelloni and Guynn, 2004; Ghosh, et al., 2013), but this match is only limited to a horizontal direction, and an examination across the whole lithospheric thickness is absent. This examination is important because it may provide valuable information on the plate driving forces. Figure 8 outlines a vertical distribution of the possible plate driving forces around the North American Plate. Geographically, the region along which the established plate driving forces (i.e., slab pull, ridge push, mantle plume) are exerted on the plate is lower than the region along which the ocean-generated force is exerted. We can expect that the stresses yielded by a combination of these driving forces and collisional resistance would concentrate in the middle and lower

parts of the plate, whereas the stresses caused by ocean-generated forces would concentrate in the upper part of the plate. With the first and second releases of stress data (Zoback et al., 1989; Zoback & Magee, 1991; Zoback, 1992), it has become clear in the WSM that the stresses manifested are mainly concentrated on the uppermost brittle part of the lithosphere. This result tends to favor the ocean-generated force rather than these established forces as the primary plate driving force. In fact, the established plate driving forces (i.e., slab pull, ridge push, mantle plume) cannot be accordance with the stress fields of the continental plate. As shown in Figure 8, these forces act on the middle and lower parts of the plate (i.e., North American Plate). Associating the motion of this plate with these forces means that the continent (i.e., North America) is being entrained by the underlying moving crust to move; that is, the underlying moving crust uses a basal shear traction to entrain the continent to move. This basal drag would result in an extensional stress that concentrates mainly along the base of the continent. Unfortunately, the WSMs released in the past 20 years generally show that the continent, which represents the upper brittle part of the continental plate, exhibits mainly compressional stress rather than extensional stress, except for some portions of the continent dominated by high topography. Subsequently, a detailed analysis of stress data found that S_{Hmax} orientations are often rotated into a plane approximately parallel to the local trend of the continental slope (Zoback et al., 1989; Zoback, 1992). Because the distributions of these established driving forces are geographically lower than that of the continent and their directions are relatively fixed, it is difficult for them to form a stress field associated with the continental slope. By contrast, the ocean-generated force is geometrically vertical to the continental slope, and it may easily form stress field associated with the continental slope. Further analysis of stress variation along the vertical direction may reveal a big discrepancy with these established plate driving forces. According to Turcotte and Schubert (2014), the push force yielded by an oceanic ridge can be written as $F_{RP}=g\rho_m\alpha_v(T_1-T_0)(1+2\rho_m\alpha_v(T_1-T_0)/(\pi(\rho_m-\rho_w))kt$, where g, ρ_m, ρ_w, T_1, T_0, and t are the gravitational constant, mantle density, water density, mantle temperature, temperature at the plate surface, and age of the oceanic plate, respectively. This expression would imply that as the density and temperature of mantle increase with depth, ridge push must increase with depth, and the lithospheric stress caused by ridge push must correspondingly increase with depth. Referring to Figure 8, the mantle plume acts on the base of the North American Plate, and there has no slab pull for this plate. Taking into account the fact that the ridge push is geographically lower and increases with depth, we may expect that a combination of ridge push, mantle plume, and collisional resistance would result in the appearance of the maximal horizontal stress in the middle and lower parts of the plate. Contrary to this expectation, an overall trend of decreasing stresses with depth has been established. The stresses (deviatoric stresses) measured in the upper parts of intraplate regions have magnitudes of 20~30 MPa

(Forsyth & Uyeda, 1975; Bott and Kusznir, 1984; Zoback & Magee, 1991). At a depth of 50~60 km from the surface, the stresses measured beneath the continent's extensional region decrease to almost 8.0 MPa. At depths of 100~200 km, which are the lower part of the continental crust, the stresses generally decrease to 15~5 MPa (Mercier, 1980; England and Molnar, 1991). By contrast, since the ocean-generated force is always exerted on the continent's side, the stress yielded by this force must concentrate mainly on the upper part of the continental plate and consequently must decrease with depth. Additionally, the pressure exerted by the ocean on a continental slope may be approximately written as $P = 0.5g\rho_w h$, where g, ρ_w, and h arethe gravitational constant, water density, and ocean depth, respectively. Given g =10 m/s, ρ_w=1000kg/m^3, and h = 5 km, the resultant pressure would be P = 25 MPa. This result matches very well with the measured stresses in the upper parts of intraplate regions (Forsyth & Uyeda, 1975; Bott and Kusznir, 1984; Zoback & Magee, 1991).

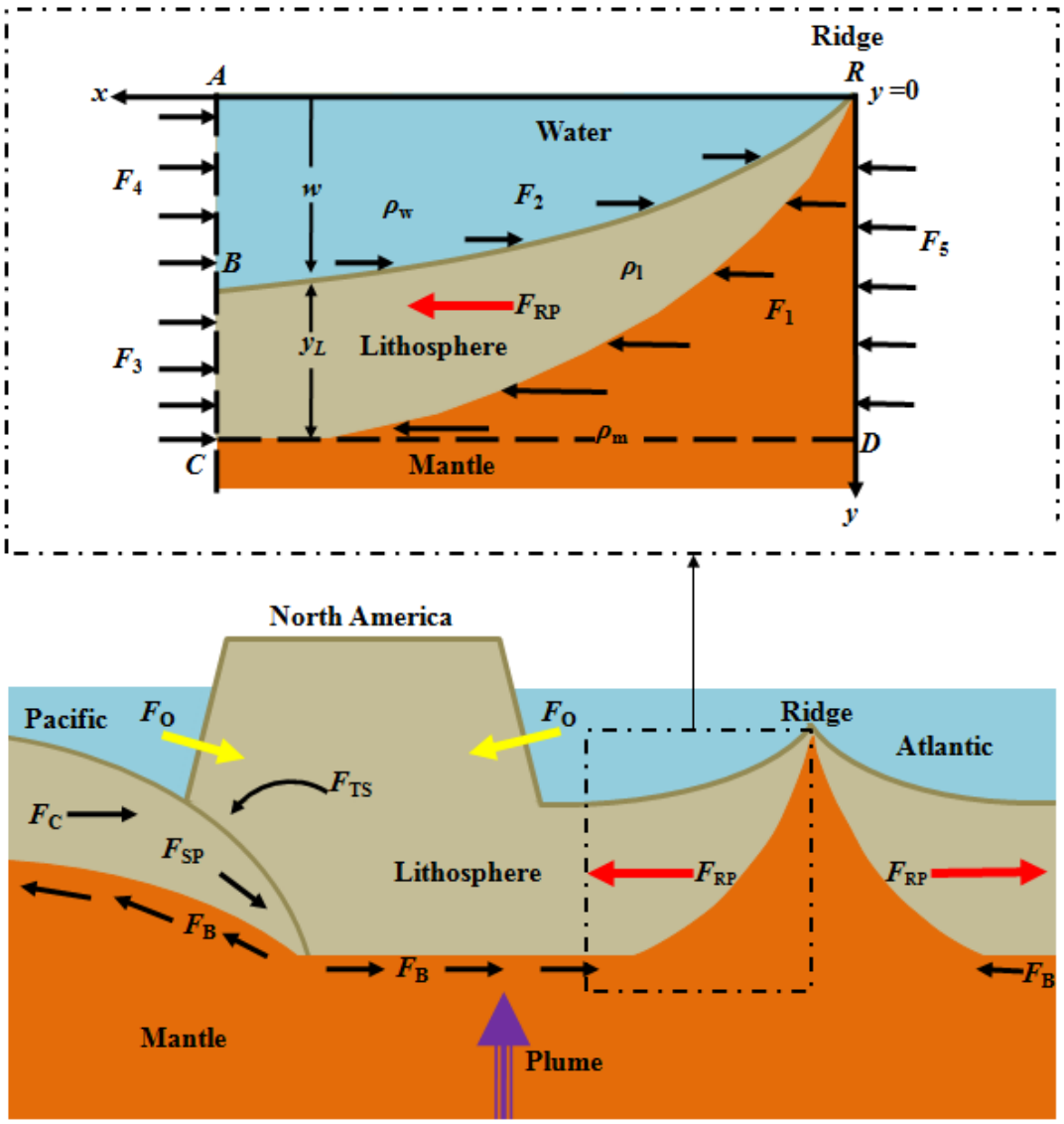

Fig. 8. Distribution of ocean-generated force and established plate driving forces. F_O, F_{RP}, F_C, F_{TS}, F_{SP}, and F_B denote the horizontal force, ridge push force, collisional resistance, trench suction, slab pull, and basal drag, respectively (if resistive). The analytic frame for ridge push refers to Turcotte and Schubert (2014).

Plotting the ocean-generated force on the WSM that was released in 2016, one feature becomes evident: the continents are uniformly compressed by the ocean-generated forces, and the stresses yielded by these forces in the continents would therefore be compressiona. Another feature is that the orientations of the ocean-generated forces around North America, South America, western Europe, Australia, China, and western Africa are dominantly subparallel to those of the stress fields over these continents (Figure 9). Associating the ocean-generated forces with these stress fields is relatively simple. For example, the ocean-generated forces compress the west, east, and northeast sides of North America, which may form predominant stresses of ENE orientation over the entire continental portion of the North American Plate. The ocean-generated forces compress the west, east, and north sides of South America, which may form predominant stresses of E-W orientation over the entire continental portion of the South American Plate. The ocean-generated forces compress western Europe, which may form a predominant stress field of NW orientation in western Europe. The ocean-generated forces compress the west, south, and east sides of Australia; together with collisional resistance from the north, a NNE stress field in central and northeastern Australia and an E-W stress field in southeastern and southwestern Australia may be created. The ocean-generated forces compress the east, southeast, and south sides of China, together with the collisional resistances from the Indian and Eurasian continents; this may form a radial pattern of stress orientations in China. The ocean-generated forces compress western Africa to form a stress field of approximately E-W orientation. The stress fields in the WSM also show that the regional and local patterns of stress fields are complicated and diverse and cannot be controlled by ridge push; these features are presently ascribed to lithospheric properties such as flexure, lateral density contrast, basin geometry, and active faulting (Sperner, et al., 2003; Heidbach, et al., 2007; Heidbach, et al., 2010). We believe that ocean-generated forces play an important role in controlling these stress patterns.

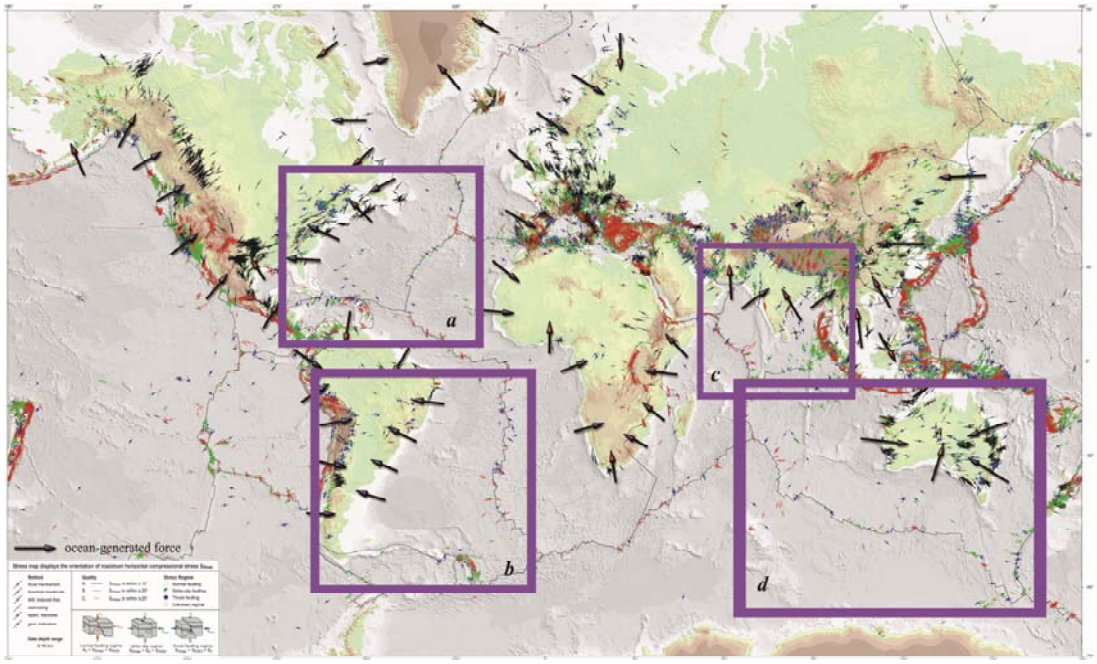

Fig. 9. Ocean-generated forces and observed stresses. The background stress map refers to Heidbach et al. (2016). Note that the stress map is formed based on a transverse Mercator projection, which leads portions of the plates to be horizontally elongated (for example, the western coastline of American continent is stretched to be nearly orthogonal to the eastern coastline); the orientations of the observed stresses therefore may not be completely correct.

3.3 Other challenges

There are other challenges for these established plate driving forces. First of all, since all plates are steadily moving over the Earth's surface, a plate in motion would naturally depart from another plate. This separation would result in a fracture between the two plates. If the fracture were deep, it would allow magma to erupt and form a mid-ocean ridge (MOR). The oceanic plates are geographically somewhat lower than the continental plates; due to this difference in elevation, the moving oceanic plates are easily subducted beneath the continental plates to form sinking slabs. In this respect, the MORs and sinking slabs themselves may be the result of plate motions. Currently, the MORs and sinking slabs are treated as the cause of the yield force and are considered to further drive the plates. This approach leads to the notorious chicken-or-egg question: which came first? In the field of physics, a movement (i.e., result) is strictly required to be separated from the force (i.e., cause) that sustains it. Second, the plates were found to have been periodically dispersed and aggregated in the distant past (Cande, et al., 1989; Cande and Kent, 1992; Ma, et al., 1996; Burchfiel, et al., 1992; Wan, 1993; Hibsch, et al., 1995), but the distributions of the sinking slabs, oceanic ridges, and mantle plumes are relatively fixed. It is therefore rather difficult to imagine how the forces yielded by these bodies can be in accordance with the periodical

dispersals and aggregations of the plates. last, the similarity in shape between the continental plate and the continent's coastline tends to contradict the notion that the driving force of the continental plate is related to the plate's boundary and the underlying mantle. As shown in Figure 9 (*a*, *b*, *c*, and *d*), the eastern coastline of the American continent is approximately subparallel to the Atlantic ridge, which is the plate's boundary, and the coastline of the Australian continent is entirely subparallel to the boundary of the Australian Plate. However, it is obvious that the length of the coastline of the American continent is larger than that of the Atlantic ridge; in particular, the length of the coastline of the Australian continent is far less than that of the boundary. This discrepancy suggests that it is the boundary (ridge) that follows the coastline rather than the coastline that follows the boundary (ridge). This pattern is also evident in the Indian Plate. This subparallel feature cannot be associated with the mantle plume because the former is located at the top of the plates, whereas the latter act on the base of the plates.

By contrast, the performance of the ocean-generated force is excellent when encountering these issues. The ocean-generated forces drive the continents to move, and the moving continents further drag the underlying crust to move, resulting in plate motion. In this process, the plate motion (i.e., the result) is clearly separated from the ocean-generated force (i.e., the cause). As the plates keep moving, the depth of the ocean basin and the orientation of the continent are adjusted accordingly, and these changes cause the magnitude of the ocean-generated force and its orientation to vary, enabling periodical dispersal and aggregation of the plates, The moving crust would therefore depart from the other crust, resulting in a fracture within crust. If the fracture occurs within an oceanic crust and if it is deep, it will allow magma to erupt and form an MOR at the boundary of the two plates. As the ocean-generated force is orthogonal to the continent's side, that is parallel to the coastline and parallel to the orientation of plate motion, the shape of the boundary between the two plates follows the shape of the coastline. For the Australian Plate, radial following around this continent's coastline results in a remarkable length difference between the plate boundary and the coastline.

4 Discussion

Plate tectonics may be a manifestation of ocean-generated force. The ocean-generated forces first drive continents to move, and the moving continents further drag the underlying crust that bears them; the moving continental crust subsequently drags the oceanic crust to which it is connected, and this sequence ultimately gives birth to plate motions around the globe. The

plate in motion would depart from, shear, and collide with other plates. The interactions between these plates may create various tectonic features (e.g., high mountain, oceanic ridge, transform fault) and activities (e.g., volcano, earthquake). A more detailed solution of these features shall be discussed in subsequent work.

The failure of earthquake prediction is widely recognized. Earthquakes arise from the fracture of plate, and this fracture is a release of tectonic stress caused by the force acting on the plate. This relationship means that, to successfully predict an earthquake, the plate driving forces must first be comprehensively understood. Our demonstration of tectonic stress reveals that these established plate driving forces (i.e., slab pull, ridge push, mantle plume) are incompetent. It is the opinion of this author that the failure to understand the plate driving force possibly contributes to the failure of earthquake prediction, and the newly proposed ocean-generated force may provide hope for improving earthquake prediction.

Many people are extraordinarily perplexed about why the Earth has plate tectonics but its twin Venus does not. Much work has shown that water provides the right conditions (maintaining a cool surface, for example) for the Earth's plate tectonics, while the loss of water on Venus prohibits plate formation (Hilairet et al., 2007; Korenaga, 2007; Lenardic and Kaula, 1994; Tozer, 1985; Hirth and Kohlstedt, 1996; Lenardic et al., 2008; Landuyt and Bercovici, 2009; Driscoll and Bercovici, 2013). This work extends such understanding: no water on Venus, no ocean-generated force, and naturally, no development of plate tectonics on the planet.

Acknowledgments We express sincere thanks to Maureen D. Long, Jeroen van Hunen, and Thorsten Becker for their helpful comments.

References

Alisic, L., et al. (2012). Multi-scale dynamics and rheology of mantle flow with plates. J. Geophys. Res., 117, B10402, doi:10.1029/2012JB009234.

Amante, C. and Eakins, B.W. (2009). ETOPO1 1 Arc-Minute Global Relief Model: Procedures, Data Sources and Analysis. NOAA Technical Memorandum NESDIS NGDC-24. National Geophysical Data Center, NOAA. doi:10.7289/V5C8276M.

Becker, T. W., Faccenna, C. (2011). Mantle conveyor beneath the Tethyan collisional belt. Earth Planet. Sci. Lett., 310, 453-461.

Becker, T. W., and O'Connell, R. J. (2001). Predicting plate velocities with mantle circulation models. Geochemistry, Geophysics, Geosystems, 2, 2001GC000171.

Bercovici, D., Tackeley, P. J., and Ricard, Y. (2015). The generation of plate tectonics from mantle dynamics. Reference Module in Earth Systems and Environmental Science: Treatise on Geophysics (Second Edition), 7, 271-318.

Bird, P., Liu, Z., Rucker, W. K. (2008). Stresses that drive the plates from below: definitions, computational path, model optimization, and error analysis. J. Geophys. Res., 113, B11406.

Bott, M. H. P. (1993). Modeling the Plate-Driving Mechanism. Journal of the Geological Society, 150, 941-951.

Bott, M. H. P. Kusznir, N. J. (1984). The origin of tectonic stress in the lithosphere. Tectonophysics,1984,105, 1-13.

Burchfiel, B. C., et al. (1992). The south Tibetan detachment system, Himalayan Orogeny: extension contemporaneous with and parallel to shortening in a collisional mountain belt. Special Paper, Geological Society of America, 269, 41.

Cande, S. C., et al. (1989). Magnetic lineations of the world's ocean basins .Tulsa, Oklahoma: American Association of Petroleum Geologists.

Cande, S. C., Kent, D. V. (1992). A new geomagnetic polarity time scale for the Late Cretaceous and Cenozoic. Journal Geophysical Research, 97(10),13917-13951.

Caldwell, P. C., Merrfield, M. A., Thompson, P. R. (2015). Sea level measured by tide gauges from global oceans — the Joint Archive for Sea Level holdings (NCEI Accession 0019568), Version 5.5, NOAA National Centers for Environmental Information, Dataset, doi:10.7289/V5V40S7W.

Cathies, L. (1971). The viscosity of the Earth's mantle, Ph.D. thesis, Princeton Univ., Princeton, N.J.

Chapple, W. M., and Tullis, T. E. (1977). Evaluation of the forces that drive the plates. J. Geophys. Res., 82, 1969-1984.

Choy, G. L., and Bowman, J. R. (1990). Rupture process of a multiple main shock sequence: Analysis of teleseismic, local, and field observations of the Tennant Creek, Australia, Earthquakes of January 22, 1988. J. Geophys. Res., 95, 6867-6882.

Cloetingh, S., and Wortel, R. (1986). Stress in the Indo-Australian plate. Tectonophysics, 132, 49-67.

Coltice, N., Gerault, M., and Ulvrova, M. (2017). A mantle convection perspective on global tectonics. Earth-Science Reviews, 165, 120-150.

Conrad, C. P., Hager, B. H. (1999). The effects of plate bending and fault strength at subduction zones on plate dynamics. J. Geophys. Res., 104, 17551-17571.

Conrad, C. P., Lithgow-Bertelloni, C. (2002). How Mantle Slabs Drive Plate Tectonics. Science, 298 (5591), 207–09.

Conrad, C. P., Lithgow-Bertelloni, C. (2004). The temporal evolution of plate driving forces: Importance of "slab suction" versus "slab pull" during the Cenozoic. J. Geophys. Res., 109, B10407, DOI:10.1029/2004JB002991.

Driscoll, P. and Bercovic, D. (2013). Divergent evolution of Earth and Venus: Influence of degassing, tectonics, and magnetic fields. Icarus. 226, 1447-1464.

England, P., Molnar, P. (1991). Inferences of deviation stress in actively deforming belts from simple physical models. Philosophical Transactions of the Royal Society, London, A337, 151-164.

Forsyth, D. & Uyeda, S. (1975). On the relative importance of the driving forces of plate motion. Geophys. J. Int., 43, 163-200.

Go¨lke, M., and Coblentz, D. (1996). Origins of the European regional stress field. Tectonophysics, 266, 11-24.

Ghosh, A., Becker, T. W., Humphreys, E. D. (2013). Dynamics of the North American continent. Geophys. J. Int., 194, 651-669.

Ghosh, A., and Holt, W. E. (2012). Plate motions and stresses from global dynamic models. Science, 335, 839-843.

Gripp, A. E., and Gordon, R.G. (2002). Young tracks of hot spots and current plate velocities. Geophysical Journal International, 150, 321-361.

Gru¨nthal, G., and Stromeyer, D. (1992). The recent crustal stress field in central Europe: Trajectories and finite element modeling. J. Geophys. Res., 97(B8), 11,805-11,820.

Hager, B. H., and O'Connel, R. (1981). A simple global model of plate dynamics and mantle convection. Journal of Geophysical Research. 86, 4843-4867.

Hager, B. H., and Richards, M. A. (1989). Long-wavelength variations in Earth's geoid: Physical models and dynamical implications. Philosophical Transactions of the Royal Society of London, Series A, 328, 309-327.

Hales, A. (1936). Convection currents in the Earth. Monthly Notice of the Royal Astronomical Society, Geophysical Supplement, 3, 372-379.

Heidbach, O., et al. (2018). The World Stress Map database release 2016: Crustal stress pattern across scales. Tectonophysics, 744,484-498.

Heidbach, O., Rajabi, M., Reiter, K. Ziegler, M., and the WSM Team. (2016). World Stress Map Database Release 2016, GFZ Data Services.

Heidbach, O., et al. (2007). Plate boundary forces are not enough: Second- and third-order stress patterns highlighted in the World Stress Map database, Tectonics, 26, http://doi.org/10.1029/2007TC002133 (PDF).

Heidbach, O., et al. (2010). Global crustal stress pattern based on the World Stress Map database release 2008. Tectonophys, 482, 3-15.

Heidbach, O., et al. (2016). World Stress Map 2016. GFZ Data Services. http://doi.org/10.5880/WSM.2016.002

Hess, H. H. (1962). History Of Ocean Basins, in Engel, A. E. J., James, H. L., & Leonard, B. F., eds. Petrologic Studies: A volume in honor of A. F. Buddington. Boulder, CO, Geological Society of America, 599-620.

Hibsch, C., et al. (1995). Paleostress analysis, a contribution to the understanding of basin tectonics and geodynamic evolution: example of the permian-cenozoic tectonics of Great Britain and geodynamic implications in Western Europe. Tectonophysics, 252, 103-136.

Hilairet, N., Reynard, B., Wang, Y., et al. (2007). High-pressure creep of serpentine, interseismic deformation, and initiation of subduction. Science, 318(5858), 1910-1913.

Hirth, G. and Kohlstedt, D. (1996). Water in the oceanic upper mantle: Implications for rheology, melt extraction and the evolution of the lithosphere. Earth and Planetary Science Letters, 144, 93-108.

Holmes, A. (1931). Radioactivity and Earth Movements. Nature, 128, 496-496.

James, T. S., Gowan, E. J., Wada, L., and Wang, K. L. (2009). Viscosity of the asthenosphere from glacial isostatic adjustment and subduction dynamics at the northern Cascadia subduction zone, British Columbia, Canada. Journal of Geophysical Research: Solid Earth,114(B4), CiteID B04405.

Jordan, T. H. (1974). Some comments on tidal drag as a mechanism for driving plate motions. J. Geophys. Res., 79, 2141-2142.

King, S. D. (1995). The viscosity structure of the mantle. In Reviews of Geophysics (Supplement) U.S. Quadrennial Report to the IUGG 1991-1994, 11-17.

Knopoff, L., and Leeds, A. (1972). Lithospheric momenta and the deceleration of the Earth. Nature, 237, 93-95.

Korenaga, J. (2007). Thermal cracking and the deep hydration of oceanic lithosphere: A key to the generation of plate tectonics? Journal of Geophysical Research 112(B5), DOI: 10.1029/2006JB004502.

Landuyt, W. and Bercovici, D. (2009). Variations in planetary convection via the effect of climate on damage. Earth and Planetary Science Letter, 277, 29-37.

Lenardic, A., Jellinek, M., and Moresi, L-N. (2008). A climate change induced transition in the tectonic style of a terrestrial planet. Earth and Planetary Science Letters, 271, 34-42.

Lenardic, A. and Kaula, W. (1994). Self-lubricated mantle convection: Two-dimensional models. Geophysical Research Letters, 21, 1707-1710.

Lithgow-Bertelloni, C., Richards, M.A. (1995). Cenozoic plate driving forces. Geophys. Res. Lett., 22, 1317-1320.

Ma, Z. J., Li, C. D., Gao, X. L. (1996). General characteristics of global tectonics in the Mesozoic and Cenozoic (in Chinese). Geological Science and Technology Information, 15(4), 21-25.

McKenzie, D. P. (1968). The Influence of the Boundary Conditions and Rotation on Convection in the Earth's Mantle. The Geophysical Journal, 15, 457-500.

McKenzie, D. P. (1969). Speculations on the Consequences and Causes of Plate Motions. The Geophysical Journal,18,1-32.

McKenzie, D. P. (1972). Plate tectonics in the nature of the solid Earth, 323-360, ed. E. C. Robertson, McGraw-Hill, New York.

Mercier, J. C. C. (1980). Magnitude of the continental lithospheric stresses inferred from rheomorphic petrology. Journal geophysical research, B,1980,85(11), 6293-6303.

Middleton, G. V., Wilcock, P. R. (1996). Mechanics in the Earth and Environmental Sciences. Cambridge University Press, Australia : pp 496.

Minster, J. B., Jordan, T. H., Molnar, P., Haines, E. (1974). Numerical modelling of instantaneous plate tectonics. Geophys. J. 36(3), 541-576.

Mitrovica, J. X. (1996). Haskell (1935) revisited. Journal of Geophysical Research, 101, 555-569.

Morgan, W. J. (1972). Deep mantle convection plumes and plate motions. Bull. A. Pet. Geol., 56, 203-213.

Mu¨ller, B., et al. (1992). Regional patterns of tectonic stress in Europe. J. Geophys. Res., 97(B8), 11,783-11,803.

Oxburgh, E. and Turcotte, D. (1978). Mechanisms of continental drift. Reports on Progress in Physics, 41, 1249-1312.

Perkeris, C. (1935). Thermal convection in the interior of the Earth. Monthly Notices of the Royal Astronomical Society, Geophysical Supplement, 3, 343-367.

Pugh, D. T. (1987). Tides, Surges and Mean Sea-Level. JOHN WILEY & SONS.

Pugh, D. T. and Woodworth, P. L. (2014). Sea-Level Science: Understanding Tides, Surges Tsunamis and Mean Sea-Level Changes. Cambridge Univ. Press, Cambridge.

Raymond, C. A., Stock, J, M., Cande, S. C. (2000). Fast Paleogene motion of the Pacific hotspots from revised global plate circuitcon straints. Geophysical Monography, 121, 359-375.

Ranalli, G. & Chandler, T. E. (1975). The Stress Field in the Upper Crust as determined from in situ Measurements. - Geol. Rundsch., 64, 653–74.

Read, H. H. & Watson, J. (1975). Introduction to Geology. New York, Halsted, pp13-15.

Richardson, R. M. (1992). Ridge Forces, Absolute Plate Motions, and the Intraplate Stress Field. Journal of Geophysical Research, 97, 11739-11748.

Richardson, R. M., and Cox, B. L. (1984). Evolution of oceanic lithosphere: A driving force study of the Nazca Plate. Journal of Geophysical Research: Solid Earth. 89 (B12), 10043-10052.

Richardson, R. M., and Reding, L. (1991). North American plate dynamics. J. Geophys. Res., 96, 12201-12223.

Richardson, R. M., Solomon, S. C., and Sleep, N. H. (1979). Tectonic stress in the plates. Rev. Geophys., 17, 981-1019.

Runcorn, S. (1962a).Towards a theory of continental drift. Nature,193, 311-314.

Runcorn, S. (1962b). Convection currents in the Earth's mantle. Nature, 195, 1248-1249.

Sharp, W. D. and Clague, D. A. (2006). 50-Ma Initiation of Hawaiian–Emperor bend records major change in Pacific plate motion. Science, 313(5791): 1281-1284.

Slomon, S. C., Sleep, N. H., and Richardson, R. M. (1975). On the forces driving plate tectonics: Inferences from absolute plate velocities and intraplate stress. Geophys. J. R. Astron. Soc., 42, 769-801.

Spence, W. (1987). Slab pull and the seismotectonics of subducting lithosphere. Reviews of Geophysics, 25 (1), 55–69.

Sperner, B., et al. (2003). Tectonic stress in the Earth's crust: advances in the World Stress Map project, in New insights in structural interpretation and modelling, edited by D. A. Nieuwland, Special Publication 212, 101-116, Geol. Soc. Spec. Pub., London.

Stadler, G., et al. (2010). The dynamics of plate tectonics and mantle flow: from local to global scales. Science, 329, 1033-1038.

Stefanick, M., and Jurdy, D. M. (1992). Stress observations and driving force models for the South American plate. J. Geophys. Res., 97, 11905-11913.

Sykes, L. R. (1967). Mechanism of earthquakes and nature of faulting on the mid-oceanic ridges. J. geophys, Res., 72, 2131-2153.

Tanimoto, T., Lay, T. (2000). Mantle dynamics and seismic tomography. Proceedings of the National Academy of Sciences, 97 (23),12409–12410.

Tozer, D. (1985). Heat transfer and planetary evolution. Geophysical Surveys, 7, 213-246.

Turcotte, D. L., and Oxburgh, E. (1972). Mantle convection and the new global tectonics. Annual Review of Fluid Mechanics, 4, 33-66.

Turcotte, D. L., Schubert, G. (2014). Geodynamics (Third Edition). Cambridge University Press, Cambridge. ISBN: 978-0-521-18623-0.

Vigny, C., et al. (1991). The Driving Mechanism of Plate Tectonics. Tectonophysics, 187, 345-360.

Vine, F. J., & Matthews, D. H. (1963). Magnetic Anomalies Over Oceanic Ridges. Nature, 199, 947-949.

Wan, T. F. (1993). Tectonic stress field and its application to the intraplate in Eastern China (in Chinese). Beijing, Geological Publishing Company, pp 1-103.

Wan, T. F. (2018). On the dynamic mechanics of global lithosphere plate tectonics (In Chinese). Earth Science Frontiers, 25, DOI:10.13745/j.esf.sf.2018.1.1.

Weatherall, P., et al. (2015). A new digital bathymetric model of the world's oceans. Earth and Space Science, 2, doi:10.1002/2015EA000107.

Wegener, A. (1915). The Origin of Continents and Oceans. New York, NY: Courier Dover Publications.

Wegener, A. (1924). The origin of continents and oceans (Entstehung der Kontinente und Ozeane). Methuen & Co.

Wessel, P. & Kroenke, L.W. (2008). Pacific absolute plate motion since 145 Ma: An assessment of the fixed hot spot hypothesis. Journal of Geophysical Research - Solid Earth 113(B6). http://dx.doi.org/10.1029/2007JB005499.

White, R., McKenzie, D. (1989). Magmatism at rift zones: The generation of volcanic continental margins and flood basalts. Journal of Geophysical Research, 94, 7685-7729.

Wilson, J. T. (1963). A possible origin of the Hawaiian Island. Canada Journal of Physics, 41, 863-868.

Wortel, R., and Cloetingh, S. (1981). On the origin of the Cocos-Nazca spreading center. Geology, 9, 425-430.

Zhong, S. (2001). Role of ocean-continent contrast and continental keels on plate motion, net rotation of lithosphere, and the geoid. J. Geophys. Res., 106, 703-712.

Zoback, M. L., and Burke, K. (1993). Lithospheric stress patterns: A global view. Eos Trans. AGU, 74, 609-618.

Zoback, M. L., et al. (1989). Global patterns of tectonic stress. Nature, 341, 291-298.

Zoback, M. L., Magee, M. (1991). Stress magnitudes in the crust: constraints from stress orientation and relative magnitude data. Philosophical Transactions of the Royal Society, London, A337(1645), 181-194.

Zoback, M. L. (1992). First- and Second-Order Patterns of Stress in the Lithosphere: The World Stress Map Project. Journal of geophysical research, 97(B8),11703-11728.

Zoback, M. D., and Zoback, M. L. (1991). Tectonic stress field of North America and relative plate motions. In Neotectonics of North America, Decade Map vol. I, edited by D. B. Slemmons et al., pp. 339-366, Geol. Soc. of Am., Boulder, Colo.